Quaternary Research xxx (2013) 586–595

Contents lists available at ScienceDirect

Quaternary Research

journal homepage: www.elsevier.com/locate/yqres

Late Pliocene–Quaternary evolution of redox conditions in the western Qaidam paleolake (NE Tibetan Plateau) deduced from Mn geochemistry in the drilling core SG-1

Yibo Yang [a], Xiaomin Fang [a,b,*], Erwin Appel [c], Albert Galy [d], Minghui Li [a], Weilin Zhang [a]

[a] Key Laboratory of Continental Collision and Plateau Uplift, Institute of Tibetan Plateau Research, Chinese Academy of Sciences, Beijing 100085, China
[b] Key Laboratory of Western China's Environmental Systems, Ministry of Education of China and College of Resources and Environment, Lanzhou University, Lanzhou 730000, China
[c] Department of Geosciences, Center for Applied Geoscience, University of Tübingen, Hölderlinstr. 12, 72074 Tübingen, Germany
[d] Department of Earth Sciences, University of Cambridge, Downing Street, Cambridge CB2 3EQ, UK

ARTICLE INFO

Article history:
Received 29 January 2013
Available online 22 August 2013

Keywords:
Late Pliocene–Quaternary
Qaidam Basin
Manganese geochemistry
Lake redox conditions
Asian inland drying

ABSTRACT

Manganese (Mn) in lake sediments reacts strongly to changes of redox conditions. This study analyzed Mn concentrations in oxides, carbonates, and bulk phases of the calcareous lacustrine sediments of a 938.5-m-long core (SG-1) taken from the western Qaidam Basin, well dated from 2.77 Ma to 0.1 Ma. Comparisons of extractions from diluted hydrochloric acid, acetic acid and citrate–bicarbonate–dithionite demonstrate that variations of Mn concentrations from acetic acid leaching (Mn_{HOAc}) are mostly responsible for Mn (II) fluctuations in the carbonate phase. Taking into account the relevant processes during weathering, transportation, deposition and post-deposition of Mn-bearing rocks, we conclude that Mn input from catchment weathering and paleolake redox condition provide the primary controls on variations in the Mn records of carbonate and oxide phases. We propose Mn_{HOAc} as a new sensitive indicator of paleolake redox evolution and catchment-scale climate change. The Mn_{HOAc} variations show a long-term upward decreasing trend, indicating a long-term decrease of Mn input from catchment weathering associated with increasing oxygen content in the paleolake bottom water. The great similarities of the Mn_{HOAc} record with other regional and global records suggest that paleolake redox changes and climatic drying in the Qaidam Basin may be largely related to global cooling.

Introduction

Manganese (Mn) in lake sediments reacts sensitively to changes in oxidation–reduction (redox) conditions. The redox behavior of Mn in lakes has been well studied and comprehensively reviewed by a number of previous researchers (e.g., Dean et al., 1981; Davison, 1993; De Vitre and Davison, 1993; Hamilton-Taylor and Davison, 1995; Wetzel, 2001). In brief, Mn is soluble in reduced phases and insoluble in oxidized ones, and readily converted in the vicinity of a redox boundary (Davison, 1993; Wetzel, 2001). Furthermore, Mn (IV) is easily reduced whereas Mn (II) does not oxidize as readily. Mn sulfides are very soluble under reducing conditions (Algeo and Maynard, 2004), and dissolved Mn is not readily taken up significantly by any organic or mineral phase (Huerta-Diaz and Morse, 1992). These two properties of Mn result in a diffuse and homogeneous distribution of Mn (II) throughout the lake water body (Hamilton-Taylor and Davison, 1995). The Mn (II) can be sequestered by carbonate formation in low Eh and slightly oxic conditions (Calvert and Pedersen, 1993; Hild and Brumsack, 1998; Caplan and Bustin, 1999; Stevens et al., 2000; Maynard, 2004; Tribovillard et al., 2006). Hence, Mn in carbonate can serve as a valuable proxy, sensitive to lake-water redox conditions. Various analyses of the geochemical dynamics of Mn and short-term Mn-bearing carbonate records have indicated that the Mn-bearing carbonates link directly to the oxygen content of the bottom water and water depth (e.g., Barnaby and Rimstidt, 1989; Huckriede and Meischner, 1996; Neumann et al., 1997; Schaller and Wehrli, 1997; Stevens et al., 2000). However, the reliability of this proxy has not yet been examined in long-term lake sediment records.

A maximum thickness of ~15,000 m of Cenozoic sediments fills the closed inland Qaidam Basin, which has an area of 12,000 km^2 and a catchment of 25,000 km^2 and is located on the northeastern Tibetan Plateau (Huang et al., 1996; Xia et al., 2001). The Cenozoic sediments consist of mudstones, calcareous mudstones and marls, intercalated siltstones, gypsum, and rock salt beds, many of which are carbonate-rich (Tuo and Philp, 2003). This site provides an excellent opportunity for studying Mn-bearing carbonates in its long-term sedimentary record. In 2008, our team carried out a deep drilling program in the central western Qaidam Basin under the Sino-German TiP-TORP projects.

* Corresponding author at: Key Laboratory of Continental Collision and Plateau uplift, Institute of Tibetan Plateau Research, Chinese Academy of Sciences, Beijing 100085, China. Fax: +86 10 8409 7079.
E-mail address: fangxm@itpcas.ac.cn (X. Fang).

0033-5894/$ – see front matter © 2013 University of Washington. Published by Elsevier Inc. All rights reserved.
http://dx.doi.org/10.1016/j.yqres.2013.07.007

A high-quality, continuous 938.5-m-long core (SG-1) was obtained with a recovery rate of 95%. High-resolution magnetostratigraphy and optically stimulated luminescence (OSL) provided ages on the core from 2.77 to 0.1 Ma (Zhang et al., 2012a). The core consists of lacustrine calcareous mudstones and siltstones intercalated with increasing salt layers upwards in the core. Analyses of pollens and spores, grain sizes and lithofacies, carbonate and salt minerals (gypsum and halite), and mineral magnetic properties have been carried out on the core material and provide considerable information on paleoclimate changes (e.g., Li et al., 2010; Wang et al., 2012 and Zhang et al., 2012a, 2012b). This investigation of the paleolake redox conditions of the SG-1 core uses the Mn geochemistry record to reconstruct paleolake water depth fluctuations and associated climate changes.

Geological setting

The Qaidam Basin lies at an elevation of about 3000 m, is the largest closed basin on the NE Tibetan Plateau, and is surrounded by the Qilian Shan (Mountains) to the north, the Kunlun Shan to the south, the Altun Shan to the west, and the Ela Shan to the east (with average elevations over 4000–5000 m; Fang et al., 2007) (Fig. 1). Mean annual temperatures, precipitation, and latent evaporation in the western basin for the past fifty years were around 2.6 °C, 17.6 mm, and 3298 mm, respectively (Li et al., 2010). This hyper-arid environment and the strongly indurated salt crust of decimeter-scale thickness prevent nearly all vegetation growth in the western part of the basin.

The basin is under northeast–southwest compression, expressed by NW–SE trending thrust faults (particularly along the Kunlun and Qilian Mountain fronts), the NW–SE oriented anticlines in the interior of the basin, and NE–SW trending strike-slip faults (Peltzer et al., 1989; Wang and Coward, 1990; Chen et al., 1999; Lowenstein and Risacher, 2009) (Fig. 1). Since the Eocene, the paleolake water has become increasingly saline, lying in a huge paleolake developed in the western end of the basin (Tuo and Philp, 2003). With the rapid movement of the Altyn Tagh fault along the Altun Shan since about late Oligocene to early Miocene, the basin was subjected to NE–SW directing compression; and the depocenter of the paleolake progressively migrated southeastwards, breaking the western basin into several sub-depressions (sub-basins). Since the Late Pliocene, the paleolake evolved into playas with climatic aridification (Chen and Bowler, 1986; Yuan et al., 1995). The westerlies provide the major climatic influence on this basin, with very minor influences from the Indian and East Asian monsoons (Fig. 1a).

Lithology and chronology of the core

The SG-1 core was drilled in a saline playa at the depocenter of the Chahansilatu sub-basin (38° 24′ 35.30″ N, 92° 30′ 32.70″ E, elevation ~2900 m), between the Eboliang anticline and the Jianshan anticline in the western Qaidam Basin (Zhang et al., 2012a, Fig. 1). The core extends 938.5 m in length with an average recovery rate of 95%. Zhang et al. (2012a) summarized the drilling; and Wang et al. (2012) and Zhang et al. (2012a) described the core lithology in detail. In brief, the penetrated sedimentary sequence consists of calcareous mudstones and siltstones, intercalated with salt layers (mainly halite) and thin or scattered gypsum crystals. Calcareous clay–siltstone layers dominate below 420 m, with some gray–white thin salt layers present at around 700 m. Cycles of thick gray–white salt and calcareous clay–siltstone layers characterize the uppermost 420 m of the sedimentary sequence (Fig. 2).

Very detailed paleomagnetic dating established ages for the core, with additional OSL dating done on the uppermost strata (Zhang et al., 2012a). In total, the ages span from 2.77 Ma to 0.1 Ma, with magnetic polarity markers obtained by the Brunhes–Matuyama boundary (at 297.9 m; 0.78 Ma), the Matuyama–Gauss boundary (at 877.5 m; 2.58 Ma), as well as using the Jaramillo (at 322.6–344.5 m; 0.99–1.07 Ma), Olduvai (at 557.0–621.9 m; 1.77–1.95 Ma), and Reunion (at 688.0 m; 2.14 Ma) normal subchrons (Zhang et al., 2012a) (Fig. 2). The lithofacies and sedimentary environment shift at a depth of about 231 m (~0.6 Ma) from the older brackish lake mudstones and perennial saline lake salt beds to younger siltstones and salt beds, locally intercalated with some thin fine sandstones deposited under saline mudflat and playa ephemeral saline lake conditions (Wang et al., 2012). These shifts may indicate some depositional hiatuses. However, the good correlation of seven cycles of both lithology (mudstone–siltstone beds and grouped salt beds) and magnetic susceptibility with those of the loess and paleosol cycles on the Chinese Loess Plateau (Zhang et al., 2012b) above the Brunhes–Matuyama boundary support the continuity of the stratigraphy on at least the ~10 ka scale. Thus our sampling at 0.5–1.5 m (equivalent to an average time of ~3–4 ka) will be sufficient for long-term geochemical and climatic studies. The depth-to-age

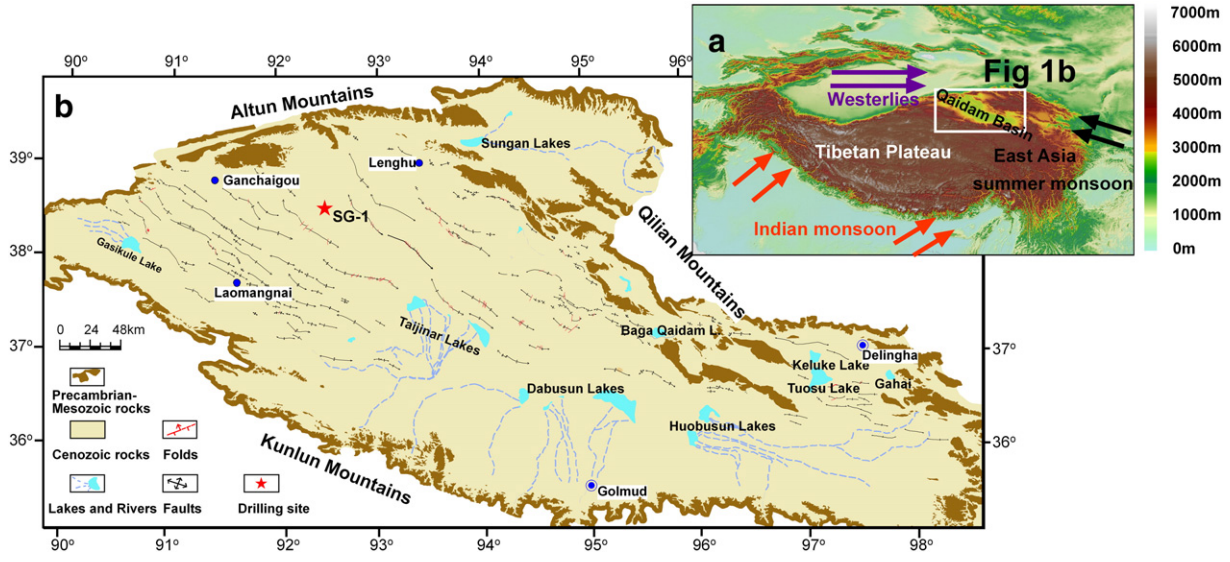

Figure 1. (a) Topographic map of the Tibetan Plateau and central Asia. (b) Map of the Qaidam Basin and adjacent regions showing the surrounding mountains, major structures, and the location of the SG-1 borehole (modified from Zhang et al. (2012b)).

https://doi.org/10.1016/j.yqres.2013.07.007 Published online by Cambridge University Press

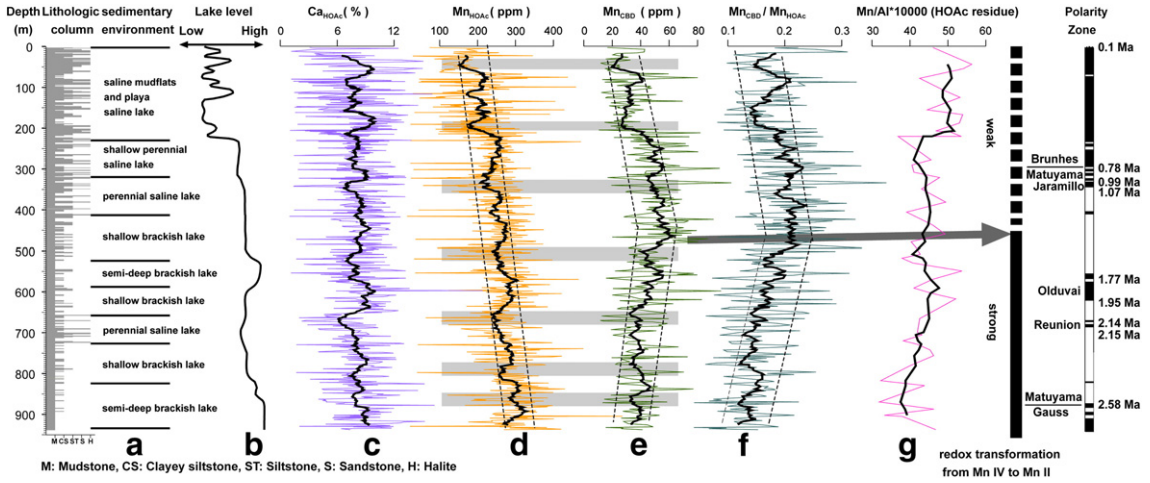

Figure 2. Depth profiles of Mn species' distributions in the SG-1 core: (a) Sedimentary environment from Wang et al. (2012); (b) The lake level fluctuation history redrawn from Wang et al. (2012); (c) Ca concentrations in the HOAc leachate (Ca_{HOAc}); (d) Mn concentrations in the HOAc leachate (Mn_{HOAc}); (e) Mn concentrations from the CBD extraction Mn_{CBD}; (f) The ratio of Mn_{CBD}/Mn_{HOAc}; and (g) The ratio of Mn/Al in the HOAc residue. Paleomagnetic results are based on Zhang et al. (2012a). The lithology column is simplified according to Wang et al. (2012). Thin lines indicate the raw data for (c–g). Bold solid lines in the records provide running averages: 25-point average for (c) and (d), 11-point for (e) and (f), and 5-point average for (g), based on the different time resolutions of each record. Thin dotted lines in (d–f) indicate the general trends for each record. The degree of redox transformation from Mn(IV) to Mn(II) is shown with the shift at the depth of 450 m.

correlation was performed by linear interpolation, using average sediment accumulation rates between the main magnetic polarity boundaries (Zhang et al., 2012a).

Materials and methods

Sampling and mineral analysis

The core sediments were sliced into 5-cm intervals directly into plastic liners, sealed in plastic sample bags in the field, and transported to Beijing for storage at 4°C. We selected a total of 805 bulk samples at various intervals (0.5–1.5 m corresponding to a resolution of ~3–4 ka) from the calcareous rocks, oven-dried them at 40°C, and ground them into fine powders.

In order to determine the major minerals (especially carbonate minerals in the core), four representative samples (two with negligible gypsum content and two with high gypsum content), were chosen for X-ray diffraction (XRD) analysis on a Rigaku D/MAX-2000 diffractometer (Cu, Ka1, 1.5406 A, 40 kV, 40 mA, 3–65°, step 0.01°, 10°/min) at the Micro Structure Analytical Laboratory, Beijing University.

Water and acid leaching

Water leaching leached away dissolved salts (halite and scattered gypsum traces; sampling of big crystals was avoided). Approximately 0.2 g of each sample was weighed into 15 ml polyethylene centrifuge tubes with 10 ml ultra-pure water. These samples were then mixed on a vortex shaker, allowed to stand for 24 h at room temperature, centrifuged, and then cleaned repeatedly three times in ultra-pure water.

Next, 10 ml 1 M acetic acid (HOAc) was added and kept at room temperature for 24 h, with occasional oscillation. Finally, the solid residues were separated by centrifuge and cleaned again three times in pure water.

In order to obtain comprehensive knowledge of the Mn species in the SG-1 core, a total of 49 HOAc solid-residue samples were oven-dried, ground into powder and digested by pressurized acid digestion using a mixture of HNO_3/HF (Li et al., 2009). In brief, 20–30 mg of the residue samples was first placed in a high-pressure Teflon digestion vessel with 1 ml concentrated HNO_3 (CMOS, JT. Baker, USA) and 1 ml concentrated HF (BVIII, Beijing Institute of Chemical Reagent Research, P.R. China). Next, the vessels were treated in an ultrasonic bath for 20 min, and then digested in an oven at 190°C for 24 h. After cooling, the solutions were dried on a hot plate at 150°C; HNO_3 was added to the residue and heated at 150°C for 24 h. Finally, the digestant was diluted to 50 ml for analysis, using ultra-pure water.

Acid extraction test

In order to detect the different effects of 1 M HOAc and 1 M HCl on the Mn extraction, 19 duplicate samples were chosen for acid leaching procedures. Wet chemical extractions are operationally defined and only moderately selective in targeting carbonate minerals, so that the results should be interpreted with caution. Due to its strong acidity, 1 M HCl dissolves carbonate phases, some Mn oxides (Chester and Hughes, 1967; van der Zee and van Raaphorst, 2004), and selectively attacks clay minerals (Chester and Hughes, 1967; Moore et al., 1997). On the other hand, 1 M HOAc is a weak acid and leaves clay minerals unaffected (Yang et al., 2000). HOAc, however, as a reducing agent, may extract some Mn oxide dissolution of any Mn-oxide coating on carbonate materials (as observed in marine sediments by Gourlan et al. (2010), although the extent of such Mn oxide dissolution is probably minor (Chester and Hughes, 1967).

Mn oxide extraction

In order to determine the Mn concentrations of free manganese oxides and oxyhydroxides, which probably exist in lake sediments (van der Zee and van Raaphorst, 2004), a total of 330 oven-dried samples were analyzed using citrate–bicarbonate–dithionite (CBD) extraction (Mehra and Jackson, 1960). Extraction was carried out twice, with a total of 1 g of sodium dithionite for each 0.5 g sample, in a hot (75 °C) Na citrate and Na bicarbonate solution (pH 7.3). The Na bicarbonate solution serves as a buffer so that no carbonates are dissolved; hence, only Mn from oxides is dissolved (Ruttenberg, 1992).

Measurements

All supernatants of the samples from each above procedure (as well as the digestant of HOAc residue) were decanted into acid-cleaned polyethylene bottles and saved for analysis. Solutions were analyzed using a Leeman Labs Prodigy-H inductively coupled plasma optical emission spectrometer (ICP–OES) at the Institute of Tibetan Plateau Research, Chinese Academy of Sciences (ITP–CAS), Beijing. Concentrations of Ca and Mn in the HOAc leachates, Mn in the CBD extractions, as well as

https://doi.org/10.1016/j.yqres.2013.07.007 Published online by Cambridge University Press

Mn and Al in the HOAc residues, are expressed in parts per million (ppm), and normalized to the weight of the bulk oven-dried sample. Replicate analyses of samples show that relative standard deviations (RSD) from the mean value were less than 2% for Ca, Mn, and Al.

Results

Mineral analysis

Evaporite minerals (halite and gypsum), carbonate minerals (calcite, aragonite and traces of dolomite), quartz, albite, muscovite, and chlorite make up the major minerals in the clastic layers (Li et al., 2010, Fig. 3). Manganese oxides and oxyhydroxides were not detected by XRD due to low concentrations and poor crystallinity (Burns and Burns, 1979). XRD did not detect any of the typical Mn carbonate minerals, such as rhodochrosite ($MnCO_3$) (as found in the sediments of Elk Lake, Minnesota; Nuhfer et al., 1993), or kutnahorite ($(Ca_{0.5}, Mn_{0.5})\ CO_3$, reported in the sediments of Big Watab Lake, Minnesota; Stevens et al., 2000). Thus, we reasonably infer that the main sources of Mn (other than Mn oxides) in the SG-1 core are Mn-bearing carbonates, mostly calcite and aragonite.

Water and acid leaching

The dissolved Mn content appears negligible, so we ignore this portion of the Mn in this study.

Mn_{HOAc} concentrations from HOAc leaching (Mn_{HOAc}) exhibit a generally decreasing trend from the bottom to the top of the core (Fig. 2d), while Ca concentrations from HOAc leaching (Ca_{HOAc}) do not (Fig. 2c). Mn_{HOAc} values range from 14 ppm to 582 ppm, with an average of 248 ppm; Ca_{HOAc} values fluctuate mostly in a range between 0.9 and 21.34 wt% (average 8.20 wt%). Mn_{HOAc} and Ca_{HOAc} concentrations clearly vary independently along the core (see the bivariate plot in Fig. 4b).

The Mn contents in the HOAc residues are expressed here by the ratio of Mn/Al, rather than the concentration (Fig. 2g). Al is a well known immobile element in chemical weathering; hence, the ratio of Mn/Al indicates the extent of gain or loss for Mn during weathering. The variations of Mn/Al in HOAc residues display a general upward increase.

The total Mn concentration (Mn_{total}) is calculated as the combination of Mn concentrations in HOAc leaching and the solid residue. Mn_{total} concentrations range from 207 ppm to 747 ppm with an average of 510 ppm, and this falls slightly below the Mn concentration of 600 ppm in the upper continental crust (Taylor and McLennan, 1985). The variations of Mn_{total} exhibit a flat trend from the bottom of the core to about 450–500 m, and then the values generally decrease above 450–500 m (Fig. 5a). Interestingly, the variations of Mn_{total} appear similar to those of Mn_{HOAc}/Mn_{total} above 450–500 m (Figs. 5a and b). Mn_{total} concentrations correlate strongly with Mn_{HOAc} (Fig. 5c).

Acid extraction test

The acid dissolution tests of selected samples (Fig. 4) show the following: (1) Mn concentrations from 1 M HCl leaching (Mn_{HCl}) range from 206 ppm to 492 ppm, with an average of 380 ppm, (which is higher than those from 1 M HOAc leaching, which range from 99 ppm to 346 ppm, with an average of 244 ppm) (Fig. 4a). Mn_{HOAc} concentrations exhibit positive correlations with Mn_{HCl} concentrations. (2) Ca concentrations from the two leaching methods yield roughly similar values, with those from HCl leaching generally slightly higher (Fig. 4c). These results indicate that both leaching methods can effectively dissolve calcite and aragonite, but that HCl has a stronger extractive ability than HOAc for other Ca-bearing minerals (e.g., dolomite) (Fig. 4c). (3) Ca and Mn concentrations extracted by the HOAc and HCl leaching do not appear related (Figs. 4b and d). (4) The differences between Mn and Ca concentrations from the two leaching methods (defined as the difference between Mn_{HCl} and Mn_{HOAc} or the ratio of Mn_{HCl} to Mn_{HOAc}, and similarly for Ca) show a weak positive correlation (Figs. 4e and f). This implies that this portion of the Mn probably results from a mixture from dissolution of dolomite, Mn oxides, and other minerals, due to the stronger dissolution capacity of 1 M HCl. (5) The Mn concentration in gypsum-rich sample follows the trend line determined by the Mn concentrations from the HOAc and HCl leaching (Fig. 4a), whereas the Ca concentration of gypsum-rich sample lies above the trend line determined by the Ca concentrations from the HOAc and HCl leaching (Fig. 4c). This indicates that the Mn concentrations in gypsum are minor compared to those in carbonate.

Extraction of Mn oxides

The Mn concentrations extracted by CBD treatment (Mn_{CBD}) increase from the bottom of the core (938.5 m) to peak values at a depth of ~450 m, followed by a subsequent decreasing trend to the top of the core (Fig. 2e). The Mn_{CBD} concentrations remain below 110 ppm (mostly <80 ppm) with an average of 46 ppm, about an order of magnitude less than Mn_{HOAc}. The most striking feature of the long-term changes of Mn_{CBD} and Mn_{HOAc} along the core can be characterized by different evolution patterns below and above 450 m (Figs. 2d

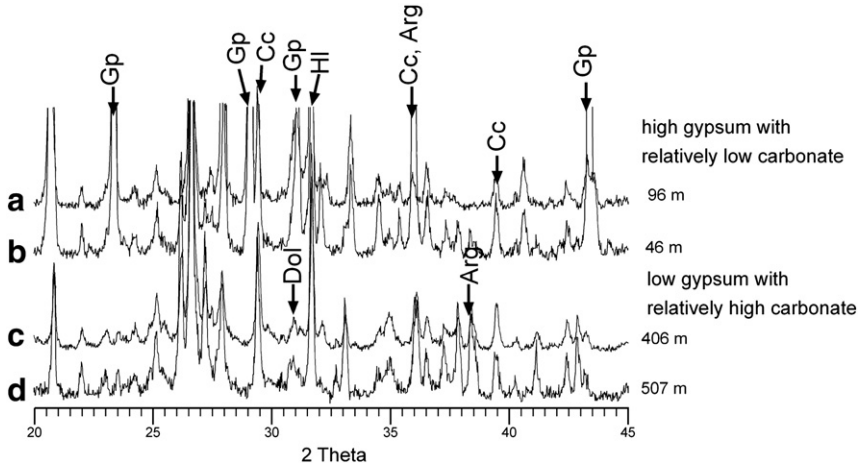

Figure 3. X-ray diffraction patterns of sedimentary minerals from four representative samples in the SG-1core. (a–b) Samples from depths 46 m and 96 m are rich in gypsum with relatively low carbonate content; (c–d) Samples from depths 406 m and 507 m have relatively high carbonate content and negligible contents of gypsum. The identified mineral peaks shown are: Arg––aragonite, Cc––calcite, Dol––dolomite, Gp––gypsum, and Hl––halite.

https://doi.org/10.1016/j.yqres.2013.07.007 Published online by Cambridge University Press

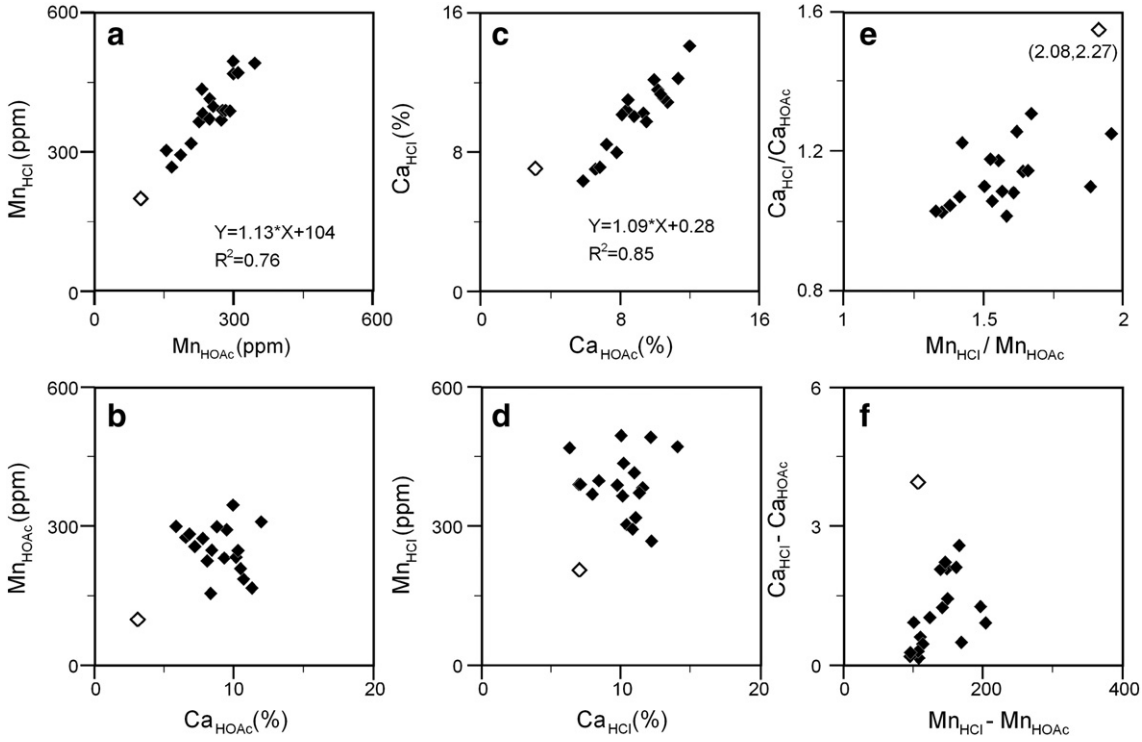

Figure 4. Scatter diagrams of Mn and Ca concentrations from 1 M HOAc and 1 M HCl extraction tests (Mn_{HCl}, Mn_{HOAc}, Ca_{HCl}, and Ca_{HOAc}): (a) Mn_{HCl} vs. Mn_{HOAc}; (b) Mn_{HOAc} vs. Ca_{HOAc}; (c) Ca_{HCl} vs. Ca_{HOAc}; (d) Mn_{HCl} vs. Ca_{HCl}; (e) (Ca_{HCl}/Ca_{HOAc}) vs. (Mn_{HCl}/Mn_{HOAc}); (f) (Ca_{HCl}–Ca_{HOAc}) vs. (Mn_{HCl}–Mn_{HOAc}). Note that the open diamond is from a gypsum-rich sample while all others are from carbonate-rich samples.

and 2e). Below 450 m the general trends of the two Mn records show roughly inverse relationships, with a poor correlation coefficient ($r^2 = 0.12$); but above 450 m they correlate positively, with a significant correlation coefficient above 450 m ($r^2 = 0.55$) (Figs. 2 and 6). However, by looking at short time-scale fluctuations superimposed on the long-term trend, we find that the major highs and lows in both Mn_{CBD} and Mn_{HOAc} records show similar (in-phase) changes (Figs. 2d and e). Furthermore, the variations of Mn_{HOAc}/Mn_{CBD} also present a two-phase pattern, decreasing upward below 450 m and tending to increase upward above 450 m (Fig. 2f).

Discussion

Geochemical interpretation

Ca_{HOAc} principally represents the calcium carbonate content in the sediments, because Ca-bearing evaporite minerals (e.g., scattered traces of gypsum; sampling of big gypsum crystals were avoided) were mostly leached away with water before the acid treatment because of their much higher solubility. However, the Ca_{HOAc} data might not entirely reflect the total carbonate content, as some dolomite was detected by XRD

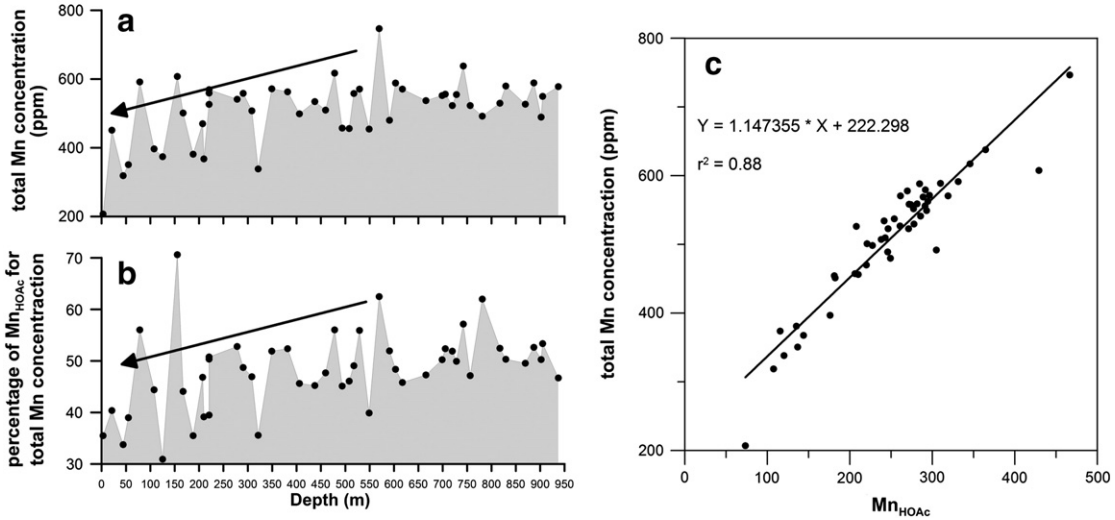

Figure 5. (a) Depth profiles of total Mn concentrations; (b) Depth profiles of percentage of Mn_{HOAc} for total Mn concentrations; (c) Scatter diagrams of Mn_{HOAc} and total Mn concentrations, showing a positive correlation. Arrows in (a) and (b) show the same general trends and oscillations of both total Mn concentrations and percentage of Mn_{HOAc} for total Mn concentrations from depths above 450–550 m.

https://doi.org/10.1016/j.yqres.2013.07.007 Published online by Cambridge University Press

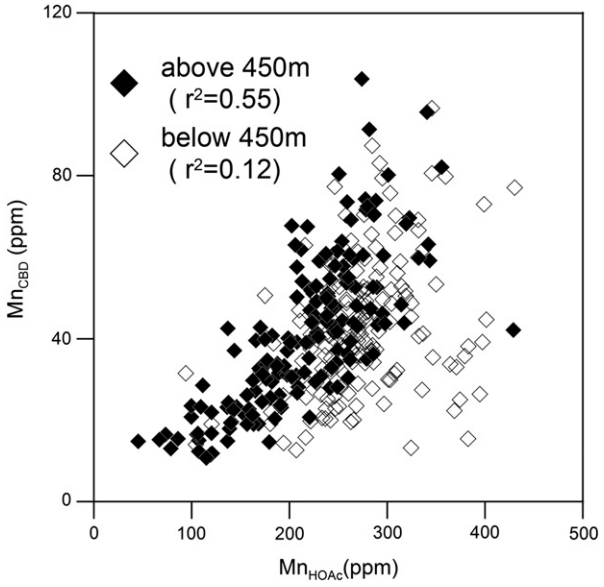

Figure 6. Scatter diagrams of Mn_{HOAc} and Mn_{CBD} above and below 450 m depth, respectively. Mn_{HOAc} and Mn_{CBD} show a positive correlation above 450 m but no clear relationship below 450 m.

in a few samples from the upper part of the core (Li et al., 2010; Fig. 4). Therefore, weak or incomplete dissolution of dolomite ($CaMg(CO_3)_2$) with 1 M HOAc may occur (Yang et al., 2000). Hence, Ca_{HOAc} concentrations mainly reflect the lower limit of the carbonate contents in the sediments, and the average Ca_{HOAc} of about 8 wt% converts to an average of 20 wt% carbonate content throughout the whole core, assuming that the 1 M HOAc leaching extracts Ca only from calcite or aragonite ($CaCO_3$).

The results of the acid leaching tests demonstrate that carbonate minerals are the dominant carriers of Mn during both HOAc and HCl leaching. Although 1 M HOAc is weaker than 1 M HCl for Mn extraction, both diluted HOAc and HCl can dissolve carbonate minerals effectively. Due to the stronger acidity, 1 M HCl will dissolve somewhat more Mn from other phases (such as oxides) than from carbonates. Based on these results, we conclude that $CaCO_3$ provides the major carrier of dissolved Mn in the reduced and calcareous sediments of the core. Even if Mn oxides are partly dissolved by 1 M HOAc, however, the contribution of Mn oxides to the Mn variations from the carbonate phases can be neglected due to low concentrations of Mn_{CBD} compared with Mn_{HOAc} in this core. We therefore attribute the variations of Mn_{HOAc} to Mn (II) in carbonate minerals, whereas the content of Mn_{CBD} mainly reflects the content of Mn oxides.

Controls on the variations of Mn_{HOAc} and Mn_{CBD} in the SG-1 core

There are several possible competing factors that may explain the Mn concentrations in the calcareous lacustrine sediments of the SG-1 core. These factors relate to the composition of the source rocks, processes releasing Mn by weathering in the source area, and other processes active during transportation, deposition, and post-deposition. First, we evaluate sources of Mn delivered into the lake from the catchment area. Then we discuss processes linked to the paleolake. Finally, we propose a model linking to the internal lake dynamics to climate changes in the drainage areas.

Sources of Mn delivered to lake

Investigations of source rock type and composition in surrounding mountains by scientists who study salt lakes in Qaidam Basin show that the exposed rocks in the drainage basin are variable with many intermediate and acid rocks. These are mainly gray gneiss, siliciclastic rocks, dolostone, quartzite, phyllite, marble, carbonatite, peridotite, serpentinite, augite, diorite, and granite of Precambrian to early Cretaceous ages (Zhang, 1987; Xuan, 1995; Wang et al., 2008). Mn-rich bedrocks, such as rhodochrosite and pyrolusite, are not found in the western Qaidam surrounding mountains (RGMRGD, 1985).

Chemical weathering of Mn-bearing rocks in the drainage area supplies the dissolved Mn load to the rivers; whereas the rivers' suspended loads predominantly contain residual alteration products, as well as secondary Mn mineral phases that formed during weathering, such as Mn oxides/oxyhydroxides. To some extent, the observed dissolved Mn, as well as secondary Mn mineral phases, represent the degree of Mn-bearing rock weathering. A warm and humid climate would likely result in much greater input of Mn released by weathering from catchments to the lakes. Hence, if no transformation from Mn oxides/oxyhydroxides to Mn (II) occurs within the lake, variations of dissolved Mn and Mn oxides/oxyhydroxides should be similar and dominantly controlled by the degree of weathering of Mn-bearing rocks in the drainage area.

Due to the larger stable Eh–pH field for Mn^{2+} (Fig. 7, Maynard, 2004), the dissolved Mn would be taken up by carbonate phase in the low Eh and slightly oxic lake water (Fig. 7). In this case, however, the dissolved Mn information would be obscured by the detrital carbonates carried into the lake. The geological setting of the paleolakes in the western Qaidam Basin has remained stable since the Late Pliocene (Chen and Bowler, 1986; Yuan et al., 1995), and that allows us to check detrital signals in this core using data from nearby locations, such as from the Lenghu and Ganchaigou sediments (see Fig. 1 for locations). The carbonate analyses of both locations (Hanson, 1999; Graham et al., 2005) show that the average proportions of the detrital carbonates to total carbonates in each locality make up only 11% and 13%, respectively. These low contents of detrital carbonates suggest that any Mn signal inherited from detrital carbonates should be relatively small.

In arid regions, eolian materials can be transported by wind into lakes and mix with aquatic sediments. Thus eolian dust provides another source of Mn input. However, the western Qaidam Basin undergoes very strong wind erosion, rather than dust accumulation, as shown by the widely distributed Yardang (wind erosion) geomorphology in the region (Kapp et al., 2011; Pullen et al., 2011). Absence of eolian loess deposition in the western Qaidam Basin confirms this (Sun, 2002).

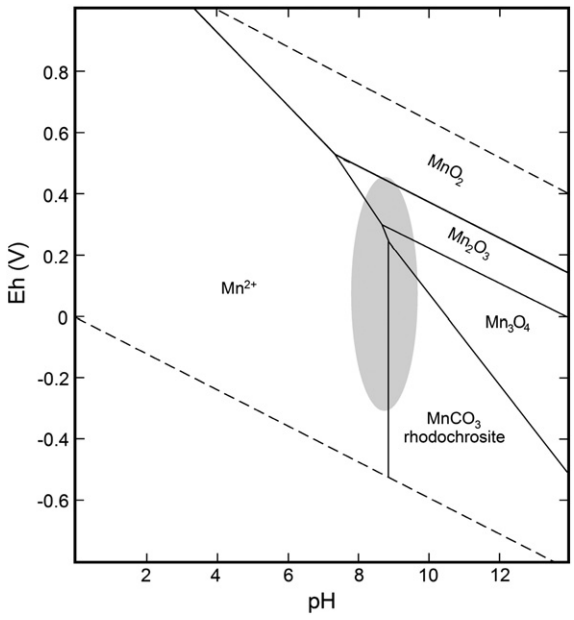

Figure 7. Eh–pH diagram showing the relationships among Mn oxides and carbonates (redrawn from Maynard (2004)). Note the large field of stability for dissolved Mn^{2+}. Rhodochrosite should be the dominant mineral at high pH under low Eh conditions. Carbonates will not exist in low pH conditions. The shaded area indicates the speculative Eh–pH field of the depositional environmental of the SG-1core, according to lithologic investigations of Wang et al. (2012).

https://doi.org/10.1016/j.yqres.2013.07.007 Published online by Cambridge University Press

Modern meteorological observations in Lenghu town (see Fig. 1 for location) demonstrate that little fine dust accumulates on cylindrical glass vessels. The coarse components account for 85% in volume, and they mostly exceed 126.4 μm (Qiang et al., 2010). Grain-size analyses of representative samples from the SG-1 core show no indicators of eolian dusts, but they do show a unique silt-size peak mode for most samples (interpreted as typical for a semi-deep lake) or a double peak (silt and fine sand) for some samples in the upper core (interpreted as small river channel deposits) (Wang et al., 2012). This exhibits a different characteristic of grain-size distribution from that of the modern eolian dust at Lenghu town (Qiang et al., 2010). Therefore, the Mn influx from eolian addition to the lake sediments in the studied region can reasonably be ignored for the purposes of this study.

Processes in the paleolake

First, we consider the precipitation of dissolved Mn, after dissolved Mn and Mn oxides/oxyhydroxides from the catchment weathering have been carried into the paleolake. The precipitation of dissolved Mn in the carbonate phase requires sufficient bicarbonate concentrations (Fig. 7). The high $CaCO_3$ contents in the core sediments indicate that sufficient bicarbonate existed in the paleolake. In that case, the Mn concentrations in carbonate phases would not be related to bulk carbonate content, but only depend on the dissolved Mn supply, because $CaCO_3$ provides an adequate carrier for dissolved Mn. The poor correlations between Ca and Mn, both from HOAc and HCl extractions (i.e., Mn_{HOAc} does not co-vary with Ca_{HOAc}) (Figs. 2, 4b and d), confirm this.

Next, we consider the paleolake redox regulation of the Mn oxides/oxyhydroxides and Mn-bearing carbonates. Although we lack a modern lake study as the reference to help explain the processes in the paleolake, the core lithology provides good indications of the processes active in paleolake systems.

The humid and warm climates in the drainage area correspond to stages of high lake levels (Wang et al., 2012). In those situations, the lithofacies in this core are characterized by gray–black laminated mudstones. The striking horizontal millimeter-scale laminations consist of alternating very thin dark clays with abundant organic matter and lighter gray silty clays or fine silts with more carbonates (Wang et al., 2012). Gray–black laminated mudstones (with occasional pyrite nodule) occur in the core, indicating lake stratification and oxygen-deficient lake bottom water (Wang et al., 2012, and their Fig. 3). Furthermore, an inverse relation between carbonates and organic matter occurs in the gray–black lamination, indicating that the geochemical processes in the paleolake resemble those in Elk Lake, Minnesota, as described by Dean (1999). The dark clays with abundant organic matter indicate a high productivity during the period of lake stratification. However, organic-matter decomposition in the hypolimnion makes the hypolimnion become anoxic, and leads to less $CaCO_3$ accumulation. During the period of the lake overturn, a larger amount of $CaCO_3$ accumulates in the sediments. Thus, in the oxygen-deficient bottom lake water, the Mn oxides/oxyhydroxides become reductively dissolved and sequestered in the carbonate phase.

When the climate becomes warm and less humid, lower lake levels and lower productivity for the paleolake can be expected. Then the greater wind shear, mixing to depth, and an unstable thermocline contribute to poor development of laminated mudstones and enhanced development of greenish gray and yellowish gray massive mudstones and siltstones (Wang et al., 2012). The observed colors change from dark gray–black to greenish gray and yellowish gray, indicating some enhanced oxidation. This most probably results from shallowing of the lake water, greater wind shear, and mixing to depth. In that case, to a lesser extent, the transformation from Mn oxides/oxyhydroxides to Mn-bearing carbonates would occur. In extreme cases, the climate becomes dry and cold, and the amount of Mn delivered by weathering would be less. The paleolake can then evolve into a shallow saline lake, like most modern saline lakes in the Qaidam Basin, with a water depth less than 1 m (Zhang, 1987). In the well-mixed and oxic lake water, reductive dissolution of Mn oxides/oxyhydroxides would hardly occur.

The issue of post-deposition alteration requires further consideration. Diagenesis of carbonate minerals can significantly alter Mn concentrations in carbonates during recrystallization. The Mn partitioning coefficients for sedimentary carbonate minerals exceed 1, meaning that Mn is preferentially incorporated into the crystals rather than the solutions (Brand and Veizer, 1980; Rimstidt et al., 1998). The carbon and oxygen isotopic results from sedimentary carbonates in the Neogene lacustrine strata from adjacent areas, such as Lenghu and Laomangnai (see Fig. 1 for locations) (Kent-Corson et al., 2009), demonstrate that the carbonate minerals are only diagenetically altered to a minor degree (Kent-Corson et al., 2009). In another way, any significant degradation of organic matter would result in CO_2 production and a decrease of pH in the pore water. And, to some extent, this pH decrease would lead to carbonate dissolution and recrystallization. Analyses of 746 samples yielded an average TOC of $0.4 \pm 0.16\%$, with a long-term upward decreasing trend (unpublished data), in accordance with climatic deterioration deduced from other proxies in this core (Li et al., 2010; Wang et al., 2012; Zhang et al., 2012b). If remarkable organic matter degradation occurs, the variation of TOC record would generally represent an upward increase, since a greater degree of organic matter degradation always happens at greater depth.

Finally, many factors influence the incorporation of Mn into carbonate, such as carbonate precipitation rates, temperature, and Mn/Ca ratios in the aqueous solutions, but these appear minor in this study. No matter how the kinetic processes change during the incorporation of Mn into carbonate, the dissolved Mn would ultimately become incorporated into carbonates. The sampling and time scales of this study allow us only to consider the bulk Mn concentrations in carbonate and force us to ignore intermediate processes during Mn partitioning.

Proposed model

All of the above processes within the catchment and lake can be synthesized by a simple conceptual model with two end-members (Fig. 8). For a lake within a closed drainage area, Mn input from both catchment weathering and lake water redox conditions relate to climate change. During periods of warm and wet climate, source rocks in the drainage area receive stronger weathering and deliver more weathering-released Mn into the lake. Under these conditions, the lake level stays high and the lake bottom water becomes oxygen-deficient, lake stratification has been strengthened. This results in a relatively high Mn content in the carbonate phase and a relatively low content of Mn oxides, due to strong transformation of Mn oxides to carbonates in the bicarbonate-rich lake water (Fig. 8a, Stevens et al., 2000). Conversely, during a period of dry and cold climate, the drainage area will receive weak weathering and deliver less weathering-released Mn into the lake. A low lake level, more oxic bottom water, and an unstable thermocline or well-mixed lake water would likely result. Because of the weak transformation from Mn oxides to carbonates in a hard water lake, both the Mn oxides and Mn content in carbonates would display similar variations (Fig. 8b).

This model could well explain the Mn_{HOAc} and Mn_{CBD} in the SG-1 core. When the paleolake bottom water was oxygen-deficient, transformation from Mn oxides to Mn carbonates would occur; however, the imprint of the original Mn oxides/oxyhydroxides input signature may be partly preserved. This could explain why the general trends of the two Mn records relate roughly inversely below 450 m, and why the short time-scale fluctuations of the two Mn records are nearly the same. During stages of less anoxic paleolake water, the redox regulation is minor. Hence, the general trends, as well as the short time scale fluctuations of the two Mn records, parallel each other.

During a period of warm and wet climate, the weathering of Mn-bearing source rocks increases, and hence Mn depletion in the residual alteration products should be substantial. If our model works, when the

https://doi.org/10.1016/j.yqres.2013.07.007 Published online by Cambridge University Press

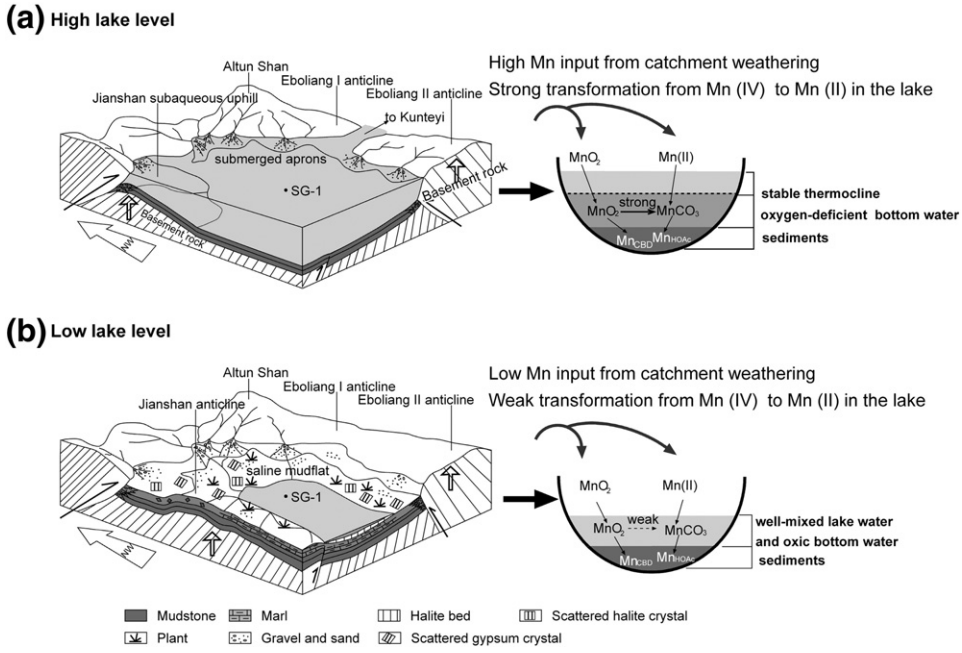

Figure 8. Conceptual model for the provenance, transportation, and deposition of Mn in the SG-1 core site: (a) a stage of high lake level with relatively warm and wet climate; and (b) a stage of low lake level with relatively dry and cold climate. The lake depositional models are redrawn from Wang et al. (2012). See text for details. Note that $MnCO_3$ herein is related to Mn precipitation in carbonate phase, and not related to rhodochrosite.

inferred climate since 2.8 Ma generally became dry and cool, an upward weakening of Mn-bearing source rock weathering, as well as a decreasing Mn depletion in the residual alteration products, is expected. If we ignore the very low Mn oxide/oxyhydroxide contents in this core, the general upward-increasing trend of Mn/Al in the HOAc residue indicates an upward decreasing trend for Mn depletion of the residual alteration products (Fig. 2g), and therefore, an upward decreased degree of Mn-bearing rock weathering in source area. This strongly confirms the applicability of our model in this region. The weakening of weathering would lead to an upward decrease in the dissolved Mn input. To some extent, the in-phase changes of Mn_{total} and Mn_{HOAc}/Mn_{total} above 450–500 m (Figs. 5a and b), as well as the positively corrected Mn_{total} and Mn_{HOAc} (Fig. 5c), clearly show the positive correlation between the degree of Mn-bearing rock weathering and the total of dissolved Mn inputs.

These two-phase, long-term changes of the Mn_{CBD} (as well as Mn_{CBD}/Mn_{HOAc}) below and above 450 m (Figs. 2e and f) occurred prior to the lithofacies shift at 414 m, from the earlier relatively brackish lake to the later restricted shallow saline lake (Wang et al., 2012, Fig. 2a). To a large extent, Mn_{CBD}/Mn_{HOAc} can serve as a proxy of Mn (IV)/Mn (II). Then, the big contrast between Mn (IV)/Mn (II) variations below and above 450 m indicates a significant reversal of the paleolake redox condition at 450 m. The depth of 450 m marks the turning point for lake water redox regulation, while the depth of 414 marks the beginning of thick salt layer appearances in the core. The lag time between these two depths seems to represent the process of decreasing lake water depth, until becoming a shallow saline lake.

Our proposed model here emphasizes both Mn input from catchment weathering as well as recycling of Mn oxides within the lake system. This is somewhat different than model proposed in Big Watab Lake, Minnesota (Stevens et al., 2000), during which the role of recycling of Mn oxides within the lake system is much more important. We think these differences are largely caused by the different surface area-to-depth ratios in Big Watab Lake and the core SG-1 paleolake. In lakes with small area-to-depth ratios (in Big Watab Lake, the surface area is only 0.9 km^2 and water depth of one subbasin is 36 m), the recycling of Mn oxides within the lake system is much more effective due to a very stable hypolimnion, and receiving Mn input from catchment weathering would play a minor role due to the small surface area. Even though the paleolake of the core SG-1 lacks a modern lake, lakes on the NE Tibetan Plateau nearly all have larger area-to-depth ratios. For example, the surface area of Lake Qinghai is more than 4260 km^2 and water depth is less than 28 m. In the modern lake, precipitation of authigenic carbonate (low-Mg calcite, aragonite, and dolomite) is in progress and lake stratification is present (LIGCAS, 1994; Jin et al., 2010). Gasikule Lake, located in the west-most Qaidam Basin (Fig. 1b), has a surface area of 103 km^2 and an average water depth of 0.65 m. Precipitation of halite is present and the lake water is oxic and well-mixed (Zhang, 1987). In those lakes with large area-to-depth ratios in our studied regions, receiving Mn input from catchment weathering would be significant due to the large surface area, and strong wind activity in the region would cause a less stable, less well-developed hypolimnion than those lakes with small area-to-depth ratios.

Paleoclimatic implications

The Mn_{HOAc} record for the bottom-water oxygen content and water-level fluctuations has been supported by the water-level reconstruction independently deduced by Wang et al. (2012) based on the different lithofacies units deposited during different water-depth environments. Wang et al.'s (2012) nine individual phases of sedimentary environments associated with corresponding lake-level fluctuations correspond with our reconstruction from the Mn_{HOAc} record (Figs. 2a, b and c). This study demonstrates the links between lake-level fluctuations, bottom-water oxidation, and climate change, as do Wang et al. (2012). Hence, Mn_{HOAc} concentrations in the SG-1 core sediments can serve as a sensitive proxy for Mn input from the catchment weathering, lake redox evolution, and climate change.

Based on the proposed model above, this long-term decrease of the Mn_{HOAc} values indicates a long-term decrease of Mn input from the catchment weathering and increasing oxidation in the lake bottom water, reflecting a long-term climate drying after 2.8 Ma. A long-term drying of central Asia since the Pliocene and Quaternary has been widely reported by many researchers from a variety of geological records: e.g., grain-size records showing the history of expansion of the Mu Us

https://doi.org/10.1016/j.yqres.2013.07.007 Published online by Cambridge University Press

Desert in northwest China (Ding et al., 2005), mass accumulation rates on the central Chinese Loess Plateau (Sun and An, 2005, Fig. 9d), and low-resolution pollen records in the western Qaidam Basin (Cai et al., 2012, Fig. 9e). However, the progression of the long-term drying remains unclear, and the lack of high-quality continuous climatic records directly from central Asia poses continuing difficulties. Our drilling sequences in the western Qaidam Basin provide new, high-quality proxy records for the region, and provide (for the first time) one continuous sequence for geochemical research.

Comparisons of the Mn_{HOAc} record from the SG-1 core with the stacked marine oxygen isotope record from benthic foraminifera (Lisiecki and Raymo, 2005, Fig. 9a) and with alkenone sea-surface temperatures of the North Atlantic Ocean (Lawrence et al., 2009, Fig. 9b) show that the Mn_{HOAc} variations generally match the global cooling and intensification of the Northern Hemisphere glaciation. The greatest similarity is observed between sea-surface temperatures of the North Atlantic Ocean and our Mn_{HOAc} record. We assume that global cooling decreases global air moisture due to reduced evaporation of oceans and continental water bodies and thus reduces the transport of moisture into the continental interior of Asia (e.g., by monsoons or the westerlies). In particular, high-latitude cooling of the Northern Hemisphere will significantly reduce moisture in the westerlies, which directly control the studied region, and will thereby lead to a drying of the Qaidam Basin, shrinking and lowering the lake, increasing oxidative conditions, and decreasing the Mn_{HOAc} content. Cooling of the high latitudes of the Northern Hemisphere has also been proposed to intensify the Siberian High (air pressure), which also affects the studied region through the enhanced westerlies (Porter and An, 1995; Fang et al., 1999) by directly adding cold air into this high pressure regime (Chen et al., 1991; Ding, 1991). An enhanced Siberian High will also give rise to a colder and drier climate for the Qaidam Basin, thus causing a decrease of the Mn_{HOAc} content.

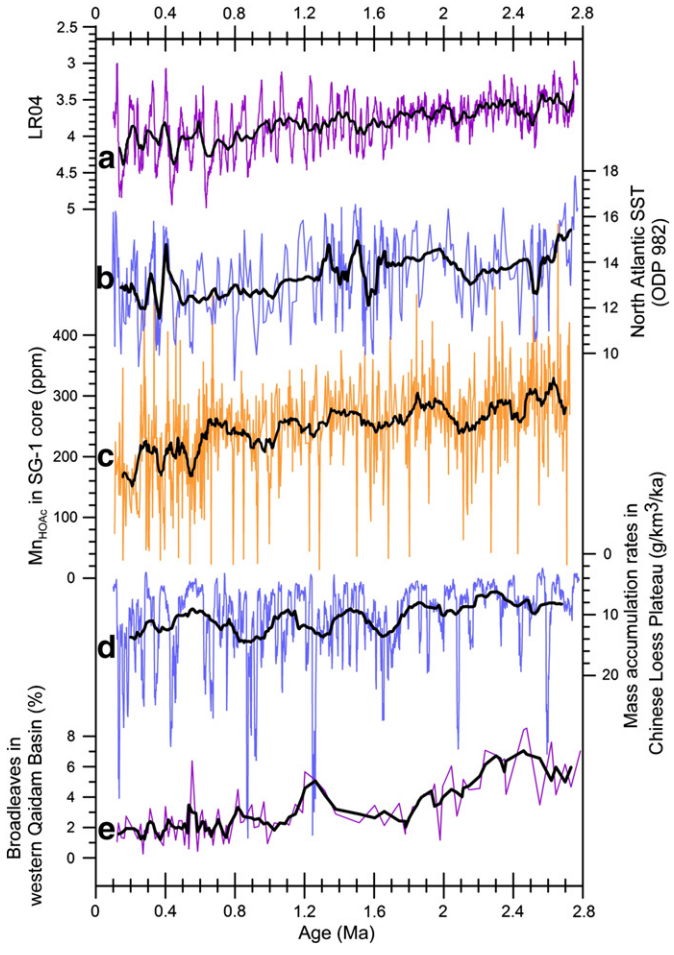

Figure 9. Comparison of the Mn_{HOAc} record of the SG-1 core (c) with other climatic records since 2.8 Ma: (a) LR04 stacked marine $\delta^{18}O$ records (Lisiecki and Raymo, 2005); (b) Alkenone-derived sea-surface temperature record from the North Atlantic Ocean at ODP Site 982 (Lawrence et al., 2009); (d) Eolian dust mass accumulation rates on the central Chinese Loess Plateau (Sun and An, 2005); and (e) Variations of broadleaf pollen content of the SG-3 core in the western Qaidam Basin (Cai et al., 2012). Bold solid lines in the records show running averages: 71-point average for (a), 21-point average for (b), 25-point average for (c), 101-point average for (d), and 3-point average for (e), all based on different time resolutions for each record.

Conclusions

1. Test experiments with HCl, HOAc, and CBD extractions demonstrate that the Mn concentration in oxides and carbonates in the anoxic, sulfate-rich, and calcareous sediments of the SG-1 core can serve as a proxy to reflect paleolake redox conditions. Carbonates (mostly $CaCO_3$) provide the major carrier of Mn (II) in the core lithology. The Ca_{HOAc} content cannot account for the Mn_{HOAc} variations; paleolake redox conditions and climate in the catchment area ultimately serve as controlling factors to the variations of Mn_{CBD} and Mn_{HOAc} in the core.
2. The 2.77 to 0.1 Ma high-resolution record obtained from the SG-1 core shows a long-term decrease of Mn_{HOAc}, suggesting a long-term decrease of Mn input from the catchment and an increase of the oxygen content in the bottom waters of the paleolake. This reflects a long-term drying of central Asia since the Late Pliocene. Global cooling, especially cooling in the high latitudes of the Northern Hemisphere, may be the major controlling factor for the paleolake evolution in the western Qaidam Basin.

Acknowledgments

This work was co-supported by the Strategic Priority Research Program of the Chinese Academy of Sciences (Grant No. XDB03020400), the National Basic Research Program of China (Grant No. 2013CB956400, 2011CB403000), the National Natural Science Foundation (NSFC grant nos. 41021001, 40920114001), the German Research Foundation (DFG) (No. AP 34/34-1 within the SPP 1372 TiP), and the German Ministry for Education and Research (BMBF) (No. 03G0705A). We are grateful to Sihu Hu, Jiyi Wang, Qibo Zhang and Yongbiao Yang for their hard work during drilling. We thank Jinbo Zan, Maotang Cai and Jiuyi Wang for the constructive discussions and Xiaoming Liu, Xiangyu Li and Shaopeng Gao for the laboratory assistance. We very much appreciate the thorough and insightful comments of the three reviewers, Walter E. Dean and another two anonymous reviewers, and the journal's Editor Derek B. Booth, Associate Editor Jay Quade, which have greatly helped to improve the manuscript. Special thanks go to Walter E. Dean, William F. Isherwood and an anonymous reviewer for their great effort in refining the English language of the manuscript.

References

Algeo, T.J., Maynard, J.B., 2004. Trace-element behavior and redox facies in core shales of Upper Pennsylvanian Kansas-type cyclothems. Chemical Geology 206, 289–318.
Barnaby, R.J., Rimstidt, J.D., 1989. Redox conditions of calcite cementation interpreted from Mn-contents and Fe-contents of authigenic calcites. Geological Society of America Bulletin 101, 795–804.
Brand, U., Veizer, J., 1980. Chemical diagenesis of a multicomponent carbonate system-1: trace elements. Journal of Sedimentary Research 50, 1219–1236.
Burns, R.G., Burns, V.M., 1979. Manganese oxides. In: Burns, R.G. (Ed.), Marine Minerals. Reviews in Mineralogy, vol. 6. Mineralogy Society of America, Washington, DC (1–46 pp.).
Cai, M., Fang, X., Wu, F., Miao, Y., Appel, E., 2012. Pliocene–Pleistocene stepwise drying of Central Asia: evidence from paleomagnetism and sporopollen record of the deep borehole SG-3 in the western Qaidam Basin, NE Tibetan Plateau. Global and Planetary Change 94–95, 72–81.
Calvert, S.E., Pedersen, T.F., 1993. Geochemistry of recent oxic and anoxic sediments: implications for the geological record. Marine Geology 113, 67–88.

Caplan, M.L., Bustin, R.M., 1999. Devonian–Carboniferous Hangenberg mass extinction event, widespread organic-rich mudrocks and anoxia: causes and consequences. Palaeogeography Palaeoclimatology Palaeoecology 149, 187–207.
Chen, K., Bowler, J.M., 1986. Late Pleistocene evolution of salt lakes in the Qaidam Basin, Qinghai Province, China. Palaeogeography Palaeoclimatology Palaeoecology 54, 87–104.
Chen, L.X., Zhu, Q.G., Luo, H.B., He, J.H., Dong, M., Feng, Z.Q., 1991. The East Asian Monsoon. Meteorological Press, Beijing (362 pp. (in Chinese)).
Chen, W.P., Chen, C.Y., Na'belek, J.L., 1999. Present-day deformation of the Qaidam Basin with implications for intra-continental tectonics. Tectonophysics 305, 165–181.
Chester, R., Hughes, M.J., 1967. A chemical technique for the separation of ferro-manganese minerals, carbonate minerals and adsorbed trace elements from pelagic sediments. Chemical Geology 2, 249–262.
Davison, W., 1993. Iron and manganese in lakes. Earth-Science Reviews 34, 119–163.
De Vitre, R., Davison, W., 1993. Manganese particles in freshwater. In: van Leeuwen, H.P., Buffle, J. (Eds.), Environmental Particles, vol. 2. Lewis, Boca Raton, pp. 317–352.
Dean, W.E., 1999. The carbon cycle and biogeochemical dynamics in lake sediments. Journal of Paleolimnology 21, 375–393.
Dean, W.E., Moore, W.S., Nealson, K.H., 1981. Manganese cycles and the origin of manganese nodules, Oneida Lake, New-York, USA. Chemical Geology 34, 53–64.
Ding, Y.H., 1991. Advanced synoptic meteorology. Meteorological Press, Beijing (792 pp. (in Chinese)).
Ding, Z.L., Derbyshire, E., Yang, S.L., Sun, J.M., Liu, T.S., 2005. Stepwise expansion of desert environment across northern China in the past 3.5 Ma and implications for monsoon evolution. Earth and Planetary Science Letters 237, 45–55.
Fang, X.M., Li, J.J., Van der Voo, R., 1999. Rock magnetic and grain size evidence for intensified Asian atmospheric circulation since 800,000 yrs B.P. related to Tibetan uplift. Earth and Planetary Science Letters 165, 129–144.
Fang, X.M., Zhang, W.L., Meng, Q.Q., Gao, J.P., Wang, X.M., King, J., Song, C.H., Dai, S., Miao, Y.F., 2007. High-resolution magnetostratigraphy of the Neogene Huaitoutala section in the eastern Qaidam Basin on the NE Tibetan Plateau, Qinghai Province, China and its implication on tectonic uplift of the NE Tibetan Plateau. Earth and Planetary Science Letters 258, 293–306.
Gourlan, A.T., Meynadier, L., Allegre, C.J., Tapponnier, P., Birck, J.L., Joron, J.L., 2010. Northern Hemisphere climate control of the Bengali rivers discharge during the past 4 Ma. Quaternary Science Reviews 29, 2484–2498.
Graham, S.A., Chamberlain, C.P., Yue, Y., Ritts, B.D., Hanson, A.D., Horton, T.W., Waldbauer, J.R., Poage, M.A., 2005. Stable isotope records of Cenozoic climate and topography, Tibetan Plateau and Tarim Basin. American Journal of Science 305, 101–118.
Hamilton-Taylor, J., Davison, W., 1995. Redox-driven cycling of trace elements in lakes. In: Lerman, A., Imboden, D.M., Gat, J.R. (Eds.), Physics and chemistry of lakes. Springer-Verlag, Berlin, pp. 217–263.
Hanson, A.D., 1999. Organic geochemistry and petroleum geology, tectonics, and basin analysis of southern Tarim and northern Qaidam, northwest China. (Ph.D. thesis) Stanford University.
Hild, E., Brumsack, H.J., 1998. Major and minor element geochemistry of Lower Aptian sediments from the NW German Basin (core Hoheneggelsen KB 40). Cretaceous Research 19, 615–633.
Huang, H.C., Huang, Q.H., Ma, Y.S., 1996. Geology of Qaidam and petroleum prediction. Geological Publishing House, Beijing (257 pp. (in Chinese)).
Huckriede, H., Meischner, D., 1996. Origin and environment of manganese-rich sediments within black shale deeps. Geochimica et Cosmochimica Acta 60, 1399–1413.
Huerta-Diaz, M.A., Morse, J.W., 1992. Pyritisation of trace metals in anoxic marine sediments. Geochimica et Cosmochimica Acta 56, 2681–2702.
Jin, Z., You, C.-F., Wang, Y., Shi, Y., 2010. Hydrological and solute budgets of Lake Qinghai, the largest lake on the Tibetan Plateau. Quaternary International 218, 151–156.
Kapp, P., Pelletier, J.D., Rohrmann, A., Heermance, R., Russel, J., Ding, L., 2011. Wind erosion in the Qaidam basin, central Asia: implications for tectonic, paleoclimate, and the source of Loess Plateau. GSA Today 21. http://dx.doi.org/10.1130/GSATG99A.1.
Kent-Corson, M.L., Ritts, B.D., Zhuang, G.S., Bovet, P.M., Graham, S.A., Chamberlain, C.P., 2009. Stable isotopic constraints on the tectonic, topographic, and climatic evolution of the northern margin of the Tibetan Plateau. Earth and Planetary Science Letters 282, 158–166.
Lawrence, K.T., Herbert, T.D., Brown, C.M., Raymo, M.E., Haywood, A.M., 2009. High-amplitude variations in North Atlantic sea surface temperature during the early Pliocene warm period. Paleoceanography 24, PA2218. http://dx.doi.org/10/1029/2008PA001669.
Li, C.L., Kang, S.C., Zhang, Q.G., Wang, F.Y., 2009. Rare earth elements in the surface sediments of the Yarlung Tsangbo (Upper Brahmaputra River) sediments, southern Tibetan Plateau. Quaternary International 208, 151–157.
Li, M.H., Fang, X.M., Yi, C.L., Gao, S.P., Zhang, W.L., Galy, A., 2010. Evaporite minerals and geochemistry of the upper 400 m sediments in a core from the Western Qaidam Basin, Tibet. Quaternary International 218, 176–189.
LIGCAS (Lanzhou Institute of Geology of Chinese Academy of Sciences), 1994. Evolution of Recent Environment in Qinghai Lake and its Prediction. Science Press, Beijing (in Chinese).
Lisiecki, L.E., Raymo, M.E., 2005. A Pliocene–Pleistocene stack of 57 globally distributed benthic $\delta^{18}O$ records. Paleoceanography 20, PA1003. http://dx.doi.org/10.1029/2005PA001164.
Lowenstein, T.K., Risacher, F., 2009. Closed basin brine evolution and the influence of Ca–Cl inflow waters: Death Valley and Bristol Dry Lake California, Qaidam Basin, China, and Salar de Atacama, Chile. Aquatic Geochemistry 15, 71–94.
Maynard, J.B., 2004. Manganiferous sediments, rocks, and ores. In: Holland, H.D., Turekian, K.K. (Eds.), Treatise on Geochemistry, volume 7 (289–308 pp.).
Mehra, O.P., Jackson, M.L., 1960. Iron oxide removal from soils and clays by a dithionite–citrate -system buffered with sodium bicarbonate. Clays and Clay Minerals 3, 317–327.
Moore, C.D., Pape, I., Tanner, B.K., 1997. Triple-axis X-ray diffraction study of polishing damage in III–V semiconductors. Nuovo Cimento Della Societa Italiana Di Fisica D-Condensed Matter Atomic Molecular and Chemical Physics Fluids Plasmas Biophysics 19, 205–212.
Neumann, T., Christiansen, C., Clasen, S., Emeis, K.C., Kunzendorf, H., 1997. Geochemical records of salt-water inflows into the deeps of the Baltic Sea. Continental Shelf Research 17, 95–115.
Nuhfer, E.B., Anderson, R.Y., Bradbury, J.P., Dean, W.E., 1993. Modern sedimentation in Elk Lake, Clearwater County, Minnesota. In: Bradbury, J.P., Dean, W.E. (Eds.), Elk Lake, Minnesota: Evidence for Rapid Climate Change in the North-Central United States, Special Paper 276. Geological Society America, Boulder (75–96 pp.).
Peltzer, G., Tapponier, P., Armijo, R., 1989. Magnitude of late quaternary left-lateral displacements along the north edge of Tibet. Science 246, 1285–1289.
Porter, S.C., An, Z.S., 1995. Correlation between climate events in the North Atlantic and China during the last glaciation. Nature 375, 305–308.
Pullen, A., Kapp, P., McCallister, A.T., Chang, H., Gehrels, G.E., Garzione, C.N., Heermance, R.V., Ding, L., 2011. Qaidam Basin and northern Tibetan Plateau as dust sources for the Chinese Loess Plateau and paleoclimatic implications. Geology 39, 1031–1034.
Qiang, M., Lang, L., Wang, Z., 2010. Do fine-grained components of loess indicate westerlies: insights from observations of dust storm deposits at Lenghu (Qaidam Basin, China). Journal of Arid Environments 74, 1232–1239.
RGMRGD (Regional Geology and Mineral Resources Geological Division of Ministry of Geology and Mineral Resources), 1985. Compilation on the Geology of Manganese Deposit in China. Geological Publishing House, Beijing (1–11 pp. (in Chinese)).
Rimstidt, J.D., Balog, A., Webb, J., 1998. Distribution of trace elements between carbonate minerals and aqueous solutions. Geochimica et Cosmochimica Acta 62, 1851–1863.
Ruttenberg, K.C., 1992. Development of a sequential extraction method for different forms of phosphorus in marine sediments. Limnology and Oceanography 37, 1460–1482.
Schaller, T., Wehrli, B., 1997. Geochemical-focusing of manganese in lake sediments–an indicator of deep-water oxygen conditions. Aquatic Geochemistry 2, 359–378.
Stevens, L.R., Ito, E., Olson, D.E.L., 2000. Relationship of Mn-carbonates in varved lake-sediments to catchment vegetation in Big Watab Lake, MN, USA. Journal of Paleolimnology 24, 199–211.
Sun, J.M., 2002. Provenance of loess material and formation of loess deposits on the Chinese Loess Plateau. Earth and Planetary Science Letters 203, 845–859.
Sun, Y.B., An, Z.S., 2005. Late Pliocene–Pleistocene changes in mass accumulation rates of eolian deposits on the central Chinese Loess Plateau. Journal of Geophysical Research-Atmospheres 110, D23101. http://dx.doi.org/10.1029/2005JD006064.
Taylor, S.R., McLennan, S.M., 1985. The Continental Crust: its Composition and Evolution. Blackwell Scientific Publications, Oxford.
Tribovillard, N., Algeo, T.J., Lyons, T., Riboulleau, A., 2006. Trace metals as paleoredox and paleoproductivity proxies: an update. Chemical Geology 232, 12–32.
Tuo, J.C., Philp, R.P., 2003. Occurrence and distribution of high molecular weight hydrocarbons in selected non-marine source rocks from the Liaohe, Qaidam and Tarim Basins, China. Organic Geochemistry 34, 1543–1558.
Van der Zee, C., Van Raaphorst, W., 2004. Manganese oxide reactivity in North Sea sediments. Journal of Sea Research 52, 73–85.
Wang, Q., Coward, M.P., 1990. The Chaidam Basin (NW China): formation and hydrocarbon potential. Journal of Petroleum Geology 13, 93–112.
Wang, C.N., Guo, X.H., Ma, M.Z., Li, J.D., Li, J., 2008. Ore-forming geological background of K–Mg Salt in Qarhan Salt Lake. Northwestern Geology 41 (1), 97–106 (in Chinese).
Wang, J.Y., Fang, X., Appel, E., Song, C., 2012. Pliocene–Pleistocene climate change at the NE Tibetan Plateau deduced from lithofacies variation in the drilling core SG-1, western Qaidam Basin. Journal of Sedimentary Research 82, 933–952.
Wetzel, R.G., 2001. Limnology: Lake and River Ecosystems, 3rd ed. Academic Press, San Diego 289–305.
Xia, W.C., Zhang, N., Yuan, X.P., Fan, L.S., Zhang, B.S., 2001. Cenozoic Qaidam Basin, China: a stronger tectonic inversed, extensional rifted basin. American Association of Petroleum Geologists Bulletin 85, 715–736.
Xuan, Z., 1995. Basic characteristic of potassium and magnesium solid deposit in Kunteyi and Mahai salt lake of Qinghai province. Journal of Salt Lake Sciences 3, 1–9 (in Chinese).
Yang, J.D., Chen, J., An, Z.S., Shields, G., Tao, X.C., Zhu, H.B., Ji, J.F., Chen, Y., 2000. Variations in $^{87}Sr/^{86}Sr$ ratios of calcites in Chinese loess: a proxy for chemical weathering associated with the East Asian summer monsoon. Palaeogeography Palaeoclimatology Palaeoecology 157, 151–159.
Yuan, J., Yang, Q., Sun, D., Huo, C., Cai, K., Wang, W., Liu, X., 1995. The Formation Conditions of the Potash Deposits in Charhan Saline Lake, Caidamu Basin, China. Geological Publishing House, Beijing (23–50 pp. (in Chinese)).
Zhang, P.X., 1987. Saline Lakes in Qaidam Basin. Science Press, Beijing (1–25 pp. (in Chinese)).
Zhang, W., Appel, E., Fang, X., Song, C., 2012a. Magnetostratigraphy of Deep Drilling Core SG-1 in the Western Qaidam Basin (NE Tibetan Plateau) and its Tectonic Implications. Quaternary Research. http://dx.doi.org/10.1016/j.yqres.2012.03.011.
Zhang, W., Appel, E., Fang, X., Yan, M., Song, C., Cao, L., 2012b. Paleoclimatic implications of magnetic susceptibility in Late Pliocene–Quaternary sediments from deep drilling core SG-1 in the western Qaidam Basin (NE Tibetan Plateau). Journal of Geophysical Research 17, B6. http://dx.doi.org/10.1029/2011JB008949.